Energies and Relativistic Corrections for the Metastable States of Antiprotonic Helium Atoms

V. I. Korobov
Joint Institute for Nuclear Research, 141980, Dubna, Russia

D. D. Bakalov
Institute for Nuclear Research and Nuclear Energy, Tsarigradsko chaussée 72, Sofia 1784, Bulgaria
(Received 16 April 1997)

We present accurate results for the energy levels of antiprotonic helium atoms with the relativistic and QED corrections of order $\alpha^4 mc^2$ taken into account. These results reduce the discrepancy between theory and experiment to about 5–10 ppm and rigorously confirm Condo's model of metastability for the long-lived fraction of antiprotonic helium. The present level of precision enables the unambiguous ascription of quantum numbers to all of the transition lines observed so far. [S0031-9007(97)04162-8]

PACS numbers: 36.10.–k, 31.15.Ar

Over the past few years a new experimental program has been launched [1] following the discovery that a fraction of the antiprotons stopped in a helium target survive for a surprisingly long time (tens of microseconds) [2]. As suggested by Condo [3] more than 20 years ago, the longevity of antiprotons in helium is explained by the existence of metastable states of the exotic atom $\mathrm{He}^+\bar{p}$. In these states the antiproton, after having substituted one of the electrons of the neutral helium atom, settles in a nearly circular orbit (n, l) with the principal quantum number n close to the value $\sqrt{M/M_e} \approx 38$, where M is the reduced mass of $\bar{p}$. The neutrality of the $\mathrm{He}^+\bar{p}$ atoms and the considerable energy difference of the order of 2 eV between sublevels with the same principal quantum number n but different orbital momentum l of the antiprotonic orbital prevent it from prompt collisional deexcitation. The internal Auger transitions are also strongly suppressed, since for large (n, l) orbitals the level spacing is much smaller than the ionization energy $I_0 = 25$ eV. The mainstream of the deexcitation process therefore occurs through radiative transitions which are slow for high values of n ($\tau \approx 1.5 \times 10^{-6}$ s).

This surprising longevity allows these states to be manipulated experimentally, e.g., by high precision measurements of laser induced transitions [4,5]. Various attempts to estimate the transition wavelengths have now been made by using the atomic configuration interaction method [6], the Born-Oppenheimer adiabatic approach [7,8], the large configuration space variational method [9], and the coupled rearrangement channel variational method [10]. The theoretical predictions clustered around the experimental values, however, with a large dispersion of 1000 pm. A substantial improvement was achieved in [11]: the nonrelativistic energies were calculated with an accuracy better than 10^{-7} a.u., which corresponds to a 1 ppm level in the nonrelativistic transition wavelengths. However, theory and experiment still disagree by 50–100 ppm indicating that further improvement is possible only by taking into consideration the relativistic and higher order QED effects.

The antiprotonic helium atom consists of three particles: a helium nucleus, an electron, and an antiproton which substitutes the second electron of the helium atom. The nonrelativistic Hamiltonian (in atomic units $e = \hbar = m_e = 1$) can be written in Jacobian coordinates as

$$H = -\frac{1}{2M}\Delta_{\mathbf{R}} - \frac{1}{2m}\Delta_{\mathbf{r}} - \frac{2}{r_{\mathrm{He}}} + \frac{1}{r_{\bar{p}}} - \frac{2}{R}, \qquad (1)$$

where $M^{-1} = M_{\mathrm{He}}^{-1} + M_{\bar{p}}^{-1}$ and $m^{-1} = m_e^{-1} + (M_{\mathrm{He}} + M_{\bar{p}})^{-1}$, $\mathbf{r}$ is the position vector of the electron with respect to the center of mass of the heavy particles, r_{He} and $r_{\bar{p}}$ are the distances from the electron to the helium nucleus and antiproton, respectively, while R is the distance between the heavy particles.

The wave function of the antiprotonic atom depends on the variables R, r, and θ (the latter being the angle between the vectors $\mathbf{r}$ and $\mathbf{R}$) and the Euler angles Φ, Θ, φ, which are separated by means of the expansion

$$\Psi_M^{L\lambda}(\mathbf{R}, \mathbf{r}) = \sum_{m=0}^{L} \mathcal{D}_{Mm}^{L\lambda}(\Phi, \Theta, \varphi) F_m^{L\lambda}(R, r, \theta), \qquad (2)$$

where $\mathcal{D}_{Mm}^{L\lambda}$ are the symmetrized Wigner D functions [11,12] of spatial parity $\lambda = (-1)^L$. It is worthwhile to note that the adiabatic solution of [7,8] belongs to the subspace of states with $m = 0$.

The functions $F_m^{L\lambda}(R, r, \theta)$ in (2) have been expanded in the form

$$F_m^{L\lambda}(R, \xi, \eta) = R^m[(\xi^2 - 1)(1 - \eta^2)]^{m/2} \times R^{l_*} \sum_n c_n R^{i_n} \xi^{j_n} \eta^{k_n} e^{-(\alpha + \beta\xi)R}, \qquad (3)$$

where $\xi = (r_{\mathrm{He}} + r_{\bar{p}})/R$ and $\eta = (r_{\mathrm{He}} - r_{\bar{p}})/R$ are the prolate spheroidal coordinates of the electron and $i_n \geq j_n$. The factor R^{l_*} is introduced to meet the requirement that the antiproton is on a nearly circular orbit.

The detailed description of the method can be found in [12].

In the case of semiadiabatic three-body systems the above method converges quickly with respect to $m_{\max} \leq L$, where $m_{\max}$ is the number of components kept

TABLE I. Energies (in a.u.) and transition wavelengths between the states $(37, 34)$ and $(36, 33)$ of the $^4\mathrm{He}^+\bar{p}$ atom for various lengths (N) of the basis set.

N	(37, 34)	(36, 33)	λ (nm)
528	−2.911 177 53	−3.007 970 98	470.7276
880	−2.911 180 36	−3.007 977 91	470.7077
1728	−2.911 180 86	−3.007 978 94	470.7051
2364	−2.911 180 90	−3.007 979 02	470.7049

in expansion (2). If $m_{\max}$ is smaller than the multipolarity of the Auger transition, the Hamiltonian projected onto this subspace has a purely discrete spectrum.

Throughout this paper we use the atomic quantum numbers (n, l) of the antiprotonic orbital to label the quantum states of the antiprotonic helium atom. Since for the states under consideration the electron is supposed to be in the ground state, the angular momentum l of the antiprotonic orbital is in one to one correspondence with the total orbital momentum L of the three-body system.

Table I illustrates the convergence of the nonrelativistic energies and the transition wavelengths obtained by the variational method of Eqs. (2) and (3). The theoretical estimate, $\lambda_{\mathrm{theor}} = 470.7049$ nm, for the wavelength of the transition $(37, 34) \to (36, 33)$, is to be compared with the experimental value, $\lambda_{\exp} = 470.724(2)$ nm [4]. Despite the high accuracy of λ_{theor}, the deviation between theory and experiment exceeds 40 ppm.

The electron in the $\mathrm{He}^+\bar{p}$ atom moves about 40 times faster than the antiproton and appears to be essentially a relativistic particle. Since the antiprotonic helium atom can be qualitatively considered as an adiabatic system and, therefore, the electron cloud density is independent of the quantum numbers n and l, one might expect that the relativistic contributions from the parent and daughter states to the transition energy strongly cancel each other. In fact, such cancellations do not really occur because the relativistic corrections have to be averaged over the antiprotonic orbitals that *do* depend on n and l.

To calculate the relativistic corrections for the bound electron we consider the electron as a Dirac particle in the electromagnetic field of two parametrically driven nuclei:

$$(E - \beta E_0)u = (\boldsymbol{\alpha} \cdot \mathbf{p} - e\varphi)u\,.$$

Applying then the *Pauli approximation*, we get the following terms that result in a shift of the energy level:

$$H_e = -\alpha^2 \frac{1}{8m^3} p^4 + \alpha^2 \left[\frac{Z_1}{8} 4\pi\delta(\mathbf{r}_{\mathrm{He}}) + \frac{Z_2}{8} 4\pi\delta(\mathbf{r}_{\bar{p}}) \right]. \tag{4}$$

Consideration of the relativistic corrections for the bound electron improves agreement between theory and experiment significantly and reduces the discrepancy to 5–10 ppm. Tables II and III, containing the nonrelativistic and relativistic energies of the the $^3\mathrm{He}^+\bar{p}$ and $^4\mathrm{He}^+\bar{p}$ metastable states, respectively, summarize the results of our numerical calculations. The schematic diagram of the transition wavelengths for the $^4\mathrm{He}^+\bar{p}$ system based on this data is presented in Fig. 1. Note that the nonrelativistic energies of Tables II and III were calculated by the same methods as in [11] but using a larger basis set with $N = 2364$, which increased the accuracy of the nonrelativistic values to about 10^{-8} a.u. In the right upper corner of these tables the states are presented with a smaller number of digits since the Auger predissociation width for these states is greater than 10^{-8} a.u.; the corresponding values were calculated by a somewhat different method as resonances in the scattering problem (see [13]). The last digit approximates the center of the resonant profile in the energy spectrum, while the width of these states is about 10 times greater than indicated by the last digit.

Comparison of the experimental and theoretical values of Table IV clearly indicates that they still disagree by a systematic shift of the order of a few ppm. To explain this shift we have to take into consideration higher order QED effects.

TABLE II. Pure Coulomb (E_c) and relativistic (E_{rel}) energies of the $^3\mathrm{He}^+\bar{p}$ atom (in a.u.).

		$v = 0$	$v = 1$	$v = 2$	$v = 3$	$v = 4$
$L = 31$	E_c	−3.348 832 11	−3.219 507 18	−3.106 142 2	−3.006 891	−2.919 764 4
	E_{rel}	−3.348 866 94	−3.219 547 43	−3.106 188 0	−3.006 942	−2.919 821 2
$L = 32$	E_c	−3.207 672 27	−3.094 450 92	−2.995 404 31	−2.908 857	−2.833 065 6
	E_{rel}	−3.207 710 68	−3.094 495 06	−2.995 454 22	−2.908 913	−2.833 126 5
$L = 33$	E_c	−3.082 114 08	−2.983 373 10	−2.897 192 26	−2.821 962 87	−2.756 217 37
	E_{rel}	−3.082 156 38	−2.983 421 38	−2.897 246 44	−2.822 022 72	−2.756 282 53
$L = 34$	E_c	−2.970 628 27	−2.884 912 60	−2.810 261 07	−2.745 174 13	−2.688 292 86
	E_{rel}	−2.970 674 76	−2.884 965 26	−2.810 319 66	−2.745 238 29	−2.688 362 11
$L = 35$	E_c	−2.871 887 14	−2.797 868 99	−2.733 508 53	−2.677 409 07	−2.628 323 99
	E_{rel}	−2.871 938 13	−2.797 926 22	−2.733 571 62	−2.677 477 50	−2.628 397 20
$L = 36$	E_c	−2.784 722 98	−2.721 165 92	−2.665 931 34	−2.617 730 54	−2.575 439 24
	E_{rel}	−2.784 778 74	−2.721 227 87	−2.665 998 94	−2.617 803 16	−2.575 516 23
$L = 37$	E_c	−2.708 090 79	−2.653 819 58	−2.606 600 23	−2.565 267 40	−2.528 834 31
	E_{rel}	−2.708 151 54	−2.653 886 33	−2.606 672 28	−2.565 344 04	−2.528 914 74

TABLE III. Pure Coulomb (E_c) and relativistic ($E_{\rm rel}$) energies of the ^{4}He$^+\bar{p}$ atom (in a.u.).

		$v = 0$	$v = 1$	$v = 2$	$v = 3$	$v = 4$
$L = 31$	E_c	−3.507 634 95	−3.364 651 64	−3.238 577	−3.127 333	
	$E_{\rm rel}$	−3.507 666 49	−3.364 688 10	−3.238 619	−3.127 380	
$L = 32$	E_c	−3.353 757 80	−3.227 676 31	−3.116 678 94	−3.019 058	−2.933 090 6
	$E_{\rm rel}$	−3.353 792 51	−3.227 716 27	−3.116 724 28	−3.019 108	−2.933 146 6
$L = 33$	E_c	−3.216 244 20	−3.105 382 64	−3.007 979 02	−2.922 444 12	−2.847 323 8
	$E_{\rm rel}$	−3.216 282 36	−3.105 426 34	−3.008 028 30	−2.922 498 91	−2.847 383 7
$L = 34$	E_c	−3.093 466 87	−2.996 335 42	−2.911 180 90	−2.836 524 54	−2.771 011 23
	$E_{\rm rel}$	−3.093 508 77	−2.996 383 11	−2.911 234 30	−2.836 583 46	−2.771 075 36
$L = 35$	E_c	−2.984 020 94	−2.899 282 16	−2.825 146 79	−2.760 233 30	−2.703 283 10
	$E_{\rm rel}$	−2.984 066 88	−2.899 334 06	−2.825 204 45	−2.760 296 41	−2.703 351 24
$L = 36$	E_c	−2.886 682 38	−2.813 115 38	−2.748 859 91	−2.692 624 82	−2.643 248 81
	$E_{\rm rel}$	−2.886 732 64	−2.813 171 69	−2.748 921 94	−2.692 692 11	−2.643 320 85
$L = 37$	E_c	−2.800 372 31	−2.736 841 18	−2.681 394 12	−2.632 832 88	−2.590 101 12
	$E_{\rm rel}$	−2.800 427 15	−2.736 902 05	−2.681 460 54	−2.632 904 28	−2.590 176 89
$L = 38$	E_c	−2.724 124 79	−2.669 551 75	−2.621 891 87	−2.580 051 39	−2.543 091 55
	$E_{\rm rel}$	−2.724 184 43	−2.669 617 27	−2.621 962 65	−2.580 126 76	−2.543 170 38

In addition to the corrections resulting from the Dirac Hamiltonian of Eq. (4), we also estimated the most important higher order relativistic and QED contributions to the energy shift, including (a) the relativistic mass correction to the kinetic energy of heavy particles:

$$H_{\rm kin} = -\alpha^2\left(\frac{\mathbf{P}_{\rm He}^4}{8M_1^3} + \frac{\mathbf{P}_{\bar{p}}^4}{8M_2^3}\right);$$

(b) the retardation of the electromagnetic field produced by the particles:

$$H_{\rm ret} = -\sum_{i\neq j}\frac{\alpha^2 Z_i Z_j}{2M_i M_j}\left[\frac{\mathbf{P}_i\mathbf{P}_j}{r_{ij}} + \frac{\mathbf{r}_{ij}(\mathbf{r}_{ij}\mathbf{P}_i)\mathbf{P}_j}{r_{ij}^3}\right];$$

(c) the leading order vacuum polarization (the Uehling potential):

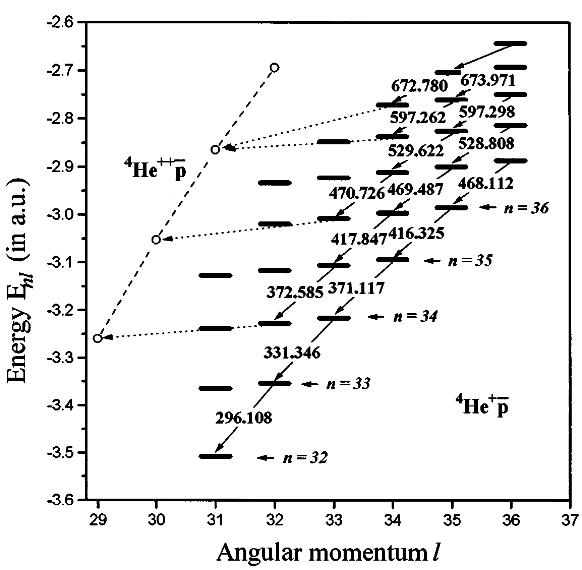

FIG. 1. Wavelengths for the favored transitions in ^{4}He$^+\bar{p}$.

$$H_{\rm VP} = \sum_{\substack{ij\\ i<j}}\frac{2Z_iZ_j\alpha}{3\pi r_{ij}}\int_1^\infty dx\,\frac{(x^2-1)^{\frac{1}{2}}(1+\frac{1}{2}x^2)}{x^2}e^{-2\gamma x r_{ij}},$$

where $\gamma = m_e c/\hbar$; (d) the interaction with electromagnetic vacuum (Welton's formula [14]):

$$H_{\rm rad} = \frac{4}{3}Z\alpha^3\ln\frac{2n^2}{(Z\alpha)^2}\delta(\mathbf{r}_{\rm He})$$

(we have to note that this is a very rough estimate); and (e) the effects of the electromagnetic structure (EMS) of the nuclei, i.e., the electromagnetic interaction of the pointlike electron with the spatially distributed electric charge of ^{4}He and $\bar{p}$ at short distances [15].

The numerical results for the state (37, 35) are presented in Table V. It is clearly seen that the dominating contribution coming from the radiative correction term (d) (i.e., from the Lamb shift for the bound electron) is only an order of magnitude smaller than the relativistic correction for the electron. Therefore, the systematic deviation between theory and experiment might be due to the radiative corrections. This work is in progress now.

TABLE IV. Comparison of the observed transition wavelengths $\lambda_{\rm exp}$ with the theoretical prediction $\lambda_{\rm theor}$ (A: pure Coulomb interaction without relativistic correction; B: with relativistic corrections). Experimental results are from [4,5, 16–18].

$(n_i, l_i) \rightarrow (n_f, l_f)$	$\lambda_{\rm exp}$ (nm)	$\lambda_{\rm theor}$ A (nm)	B (nm)	Ref.
^{4}He (39, 35) → (38, 34)	597.259(2)	597.229	597.262	[4]
^{4}He (38, 35) → (37, 34)	529.621(3)	529.596	529.623	[17]
^{4}He (37, 34) → (36, 33)	470.724(2)	470.705	470.725	[5]
^{3}He (38, 34) → (37, 33)	593.388(1)	593.360	593.393	[16]
^{3}He (36, 33) → (35, 32)	463.946(2)	463.928	463.949	[16]
^{4}He (37, 34) → (38, 33)	713.578(6)	713.520	713.593	[18]
^{4}He (37, 35) → (38, 34)	726.095(2)	726.021	726.102	[18]

TABLE V. Contribution of various relativistic and QED terms to the energy shift of the $(37, 35)$ state of $^4He^+\bar{p}$.

$\delta_e(E) \sim 0.5 \times 10^{-4}$ a.u.
$\delta_{\rm rad}(E) \sim 0.6 \times 10^{-5}$ a.u.
$\delta_{\rm VP}(E) \sim 0.4 \times 10^{-6}$ a.u.
$\delta_{\rm kin}(E) \sim 0.3 \times 10^{-7}$ a.u.
$\delta_{\rm ret}(E) \sim 0.3 \times 10^{-7}$ a.u.
$\delta_{\rm ems}(E) \sim 1.5 \times 10^{-9}$ a.u.

During the last year new experimental techniques were introduced that enabled the study of a much wider class of metastable states. In these experiments the laser was tuned to the wavelength predicted by theory and new resonances were found almost immediately after starting the scan [19]. This thoroughly confirms the accuracy of the present theoretical approach.

Through the study of the fine and hyperfine structure of antiprotonic helium atoms it is also expected to obtain valuable information on the electromagnetic structure of antiprotons, as a part of a general program to investigate the fundamental properties of antiprotons. We hope that this goal can be achieved since the success in studying the helium fine structure proves that QED can be tested with high precision even for a system which has no analytical solution [20]. The first experimental results on the fine structure of antiprotonic helium atoms [21] are encouraging.

The authors express their deep gratitude to Professor T. Yamazaki for the numerous discussions and indispensable help while carrying out this work and for making experimental results available prior to publication. We are also greatly indebted to Dr. J. Eades for comments on the manuscript. This work has been partially supported by National Science Foundation Grant No. INT-9602189, which is gratefully acknowledged.

[1] T. Yamazaki *et al.*, Nature (London) **361**, 238 (1993).
[2] M. Iwasaki *et al.*, Phys. Rev. Lett. **67**, 1246 (1991).
[3] G. T. Condo, Phys. Lett. **9**, 65 (1964).
[4] N. Morita *et al.*, Phys. Rev. Lett. **72**, 1180 (1994).
[5] F. Maas *et al.*, Phys. Rev. A **52**, 4266 (1995).
[6] T. Yamazaki and K. Ohtsuki, Phys. Rev. A **45**, 7782 (1992).
[7] I. Shimamura, Phys. Rev. A **46**, 3776 (1992).
[8] P. T.Greenland and R. Thürwächter, Hyperfine Interact. **76**, 355 (1993).
[9] O. I. Kartavtsev, in *Proceedings of the Third International Symposium on Muon and Pion Interaction with Matter*, edited by T. N. Mamedov and V. N. Duginov (JINR, Dubna, 1995), p. 138.
[10] Y. Kino (unpublished).
[11] V. I. Korobov, Phys. Rev. A **54**, 1749 (1996).
[12] V. I. Korobov, I. V. Pusynin, and S. I. Vinitsky, Muon Catal. Fusion **7**, 63 (1992).
[13] V. I. Korobov and I. Shimamura (to be published).
[14] A. A. Sokolov, I. M. Ternov, and V. Ch. Zhukovsky, *Kvantovaya Mehanika* (Nauka, Moscow, 1979) (in Russian).
[15] D. Bakalov, Yad. Fiz. **48**, 335 (1988) [Sov. J. Nucl. Phys. **48**, 210 (1988)].
[16] H. A. Torii *et al.*, Phys. Rev. A **53**, R1931 (1996).
[17] R. S. Hayano *et al.*, Phys. Rev. A **55**, 1 (1997).
[18] T. Yamazaki *et al.*, Phys. Rev. A **55**, R3295 (1997).
[19] B. Ketzer *et al.*, Phys. Rev. Lett. **78**, 1671 (1997).
[20] F. M. J. Pichanick and V. W. Hughes, in *Quantum Electrodynamics*, edited by T. Kinoshita (World Scientific, Singapore, 1990).
[21] E. Widmann *et al.*, Phys. Lett. B **404**, 15 (1997).